Lasers in Manufacturing Conference 2025

Ultrashort pulsed laser robot system: Realization of a concept for large area 3D micromachining

Yongting Yang[a,*], Daniel Franz[a], Cemal Esen[b], Ralf Hellmann[a]

[a] *Applied Laser and Photonics Group, University of Applied Sciences Aschaffenburg, Würzburger Str. 45, 63739 Aschaffenburg, Germany*
[b] *Applied Laser Technologies, Ruhr-University Bochum, Universitätsstraße 150, 44801 Bochum, Germany*

Abstract

We report on an ultrashort pulsed laser robot system, wherein an ultrashort pulsed laser is integrated on an axis of a six-axis articulated industrial robot. The combined motion of a 2D galvanometer scanner and the robot enhances the processing flexibility of 2D ultrashort pulse laser micromachining while extending the processing capabilities to true three-dimensions. CMOS cameras are mounted on the individual axes to monitor the beam center positions during or after robot movement. An adaptive beam stabilization system for beam position misalignment suppression is demonstrated to effectively reduce beam position misalignment within defined tolerances. With defining beam focus as the tool center point, the system reaches a 710 mm×960 mm×560 mm processing area. A set of selected large area 2D and 3D micromachining applications using the ultrashort pulsed laser robot system demonstrates its capability for flexible ultrashort pulsed laser processing. In addition, a real 3D ultra-thin glass cutting application highlights the system advantages on micromachining for the complex structures.

Keywords: laser robot; ultrashort pulsed laser robot; ultra-short pulse laser application; 3D micromachining;

1. Introduction

Ultrashort pulsed lasers (USPs) deliver high optical intensities with pulse durations in the femtosecond to picosecond range. Predominant non-thermal mechanisms such as multiphoton ionization and avalanche ionization enable highly controlled material processing while significantly suppressing heat-affected zones. The rapid advancements in laser technology combined with sophisticated beam delivery systems and computational modelling have significantly broadened the applications of USPs (Raciukaitis, 2021). Most of current laser processing techniques, such as, e.g., fine cutting (Mishchik, 2016), micro drilling (Franz et al., 2022), laser direct writing (Belle et al., 2022), material modification (Bischoff et al., 2023) and laser turning (Zettl et al., 2021) rely on conventional 2D or 2.5D machine concepts. However, these approaches face challenges in meeting the growing demand for fabricating intricate 3D geometries with high precision.

(Batal et al., 2020) realized a laser induced surface structure on the surface of a 3D printed Ti-6Al-4V spherical shell. The authors applied adjusted laser focus offset distance and beam incidence angle as well as surface tessellation with respect to the real surface curvature for geometry segmentation and laser scanning path calculation. The surface was manufactured by a 310-fs laser system and a 5 degree of freedom mechanical stage and a 2D beam deflection system with a telecentric F-Theta lens. Furthermore, (Karkantonis et al., 2022) analyzed the processing performance of simultaneous multi-axis USP laser micromachining. The authors applied scribing processing on a spherical aluminum shell in 4 scanning directions and found that the process uncertainty was line length error 11 µm, line spacing error 2.02 µm, angle error of 0.72º, respectively. In addition, 3D beam shaping has been proposed as a promising solution to overcome the challenges associated with 3D micromachining using USP lasers. By applying diffractive optical elements, the beam shape and focal length are precisely controlled, enabling enhanced precision and flexibility in micromachining processes (Brodsky and Kaplan, 2022).

However, the existing 3D processing methodologies are constrained in their ability to accommodate large geometries. To enable highly flexible and precise 3D micromachining, a novel concept for ultrashort pulsed laser processing has been developed. This concept involves the integration of a USP laser with an articulated six-axis industrial robot, namely an

ultrashort pulsed laser robot (USPLR) system (Franz et al., 2023). The system characteristics are discussed, and an adaptive beam guidance is presented subsequently in this contribution. Finally, applications of large area 2D and 3D micromachining using the USPLR system for different materials are presented.

2. Experimental

The USPLR system consists of a six-axis articulated industrial robot (IRB 2600ID-8/2.00, ABB) and a USP laser (CB3-40W, Light Conversion) integrated on the third robot axis (Fig. 1). The laser beam is guided by mirrors from A3 to A6. Two 2D galvanometer deflectors (RTAX-A15 and RT AY-A15, Newson) and a telecentric F-theta lens with a focal length of 160 mm (JENar Silverline F-Theta, Jenoptik) on A6 are used for deflecting and focusing the laser beam, respectively. Four CMOS cameras (2x DMK 37AUX250, 2x DMK 38UX541, The Imaging Source) on A3 to A6 monitor beam center position. The mirrors with piezoelectrical inertial actuators (PMs) and cameras (CAM3 and CAM4) contribute to a beam stabilization system (Yang et al., 2023, 2025). Piezoelectrical inertial actuators (PIAK10, Thorlabs) align mirrors (PM1 and PM2) in the x and y direction

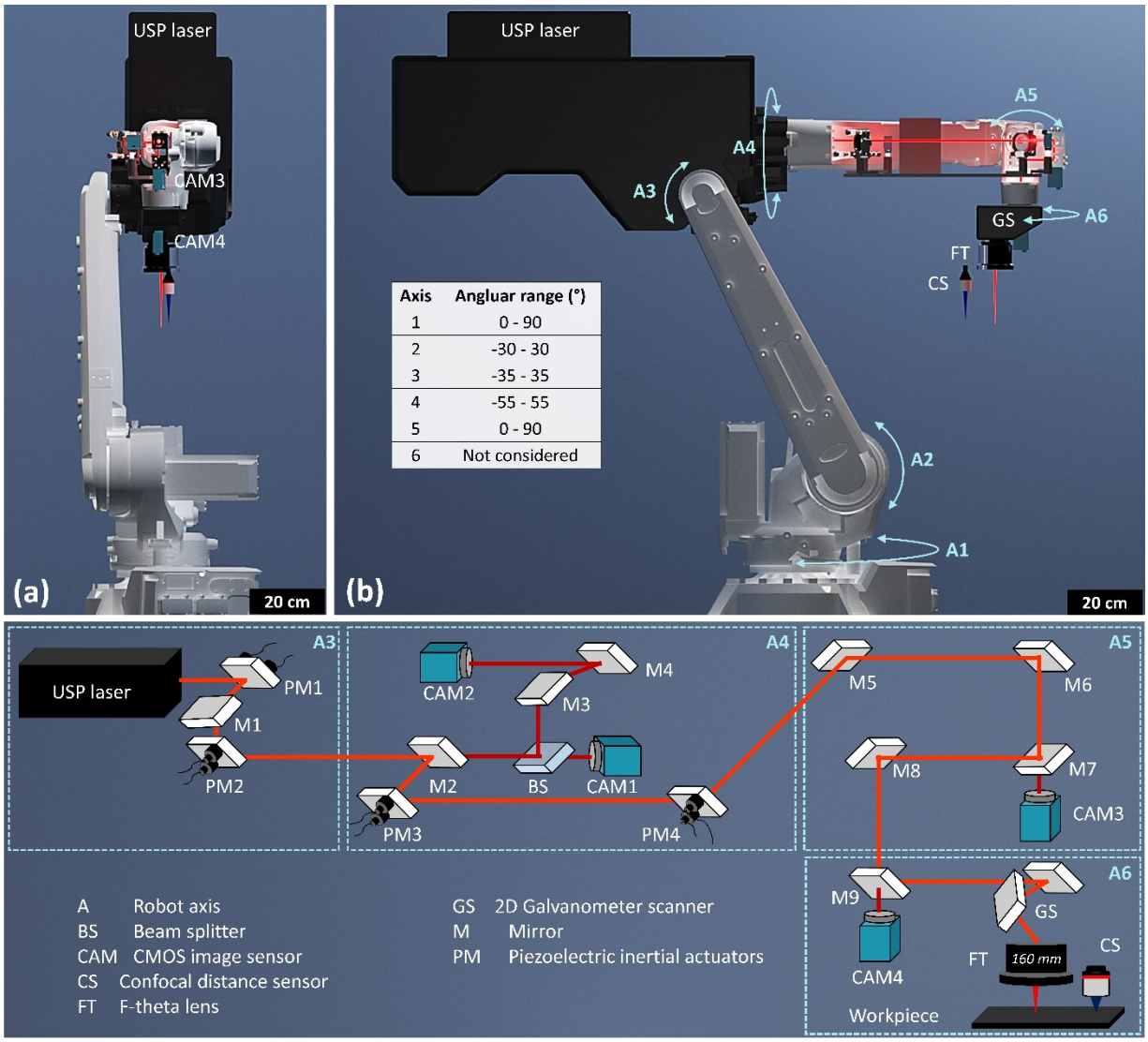

Fig. 1 Illustration of the USPLR system. A 2D galvanometer scanner and a telecentric F-theta lens are used to deflect and focus the laser beam within the focal plane, respectively. Cameras are integrated on the robot axes to detect the dynamic laser beam position. A beam stabilization consisting of mirrors aligned by piezoelectric inertial actuators and cameras is applied to correct the beam position misalignment. A confocal distance sensor is used for monitoring and adjusting the distance between the beam focus and workpiece surface. (a) Front view. (b) Side view. (c) Schematic of the optical beam path. (Franz et al., 2023, Yang et al., 2023)

for correcting the detected beam position misalignment. In addition, a confocal distance sensor (CL-L070, Keyence) is applied for monitoring the laser focus distance from the workpiece surface, which is also suitable for transparent materials.

3. Results and Discussion

3.1. Characterization of beam path on the USPLR system

First, the influence of single axial rotation is analyzed. The beam position deviations captured by cameras fixed on A5 are represented in the x and y directions (Fig. 2(a)). Axis A1 exhibits an average position deviation of 10.3 µm and a standard deviation of 5.1 µm, which yet contributes negligibly to the beam position deviation because the USP laser is integrated on the axis behind A1. Nevertheless, the influence of A2 and A3 is still notable. The primary cause of this deviation is the deformation of the carbon housing on axis A3, which is attributable to disparate leverage effects on the USP laser, consequently inducing the laser beam misalignment. The maximum beam position deviation is observed on A5 movement, yielding a high average deviation of up to 1771.6 µm with a standard deviation of 1503.4 µm in the y direction on CAM4. The reason here is the cumulative influence of mechanical backlash in the joints and the distinct center of mass for each axis.

The influence of system complex movement is studied by a combined motion of A4 and A5. The A4 rotates to the position of -45°, 0° and 45° with a superimposed movement of axis A5 in the range of 0° to 90 in 2.5° increments. After A5 arrived at each defined position, a grayscale image is captured by CAM3 and CAM4. As shown in Fig. 2(b), a higher beam position deviation is observed on CAM4, the beam position deviation during the movement of A5 tends to a similar arc shape at all the A4 positions.

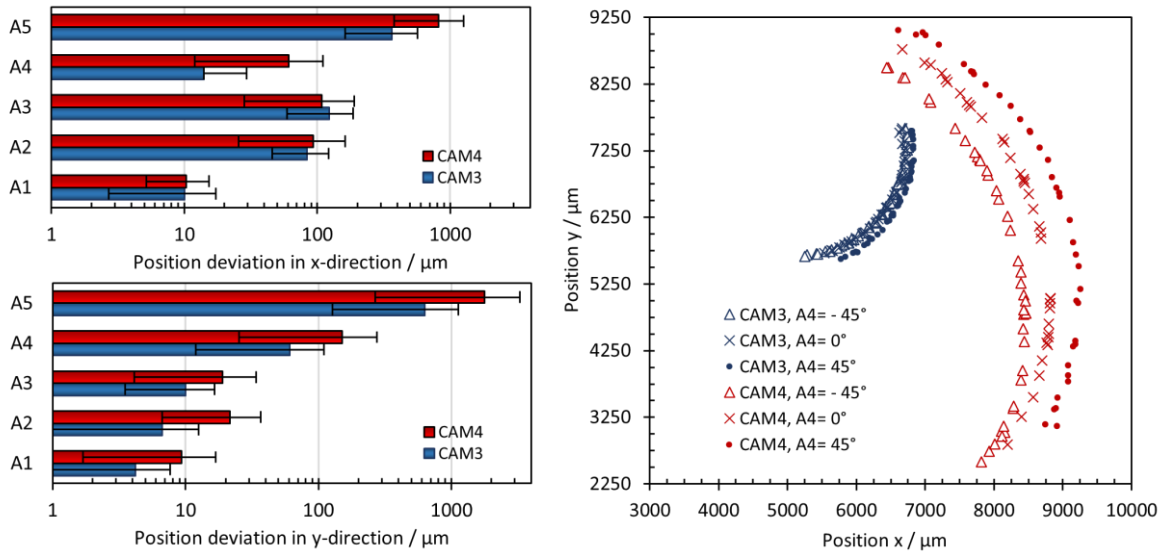

(a) (b)

Fig. 2 Dynamic laser beam positioning. (a) Average value of beam center (FWHM) position misalignment from the initial position after single movement of A1-A5. (b) Beam center position distribution during the combined movement of A4 on the position of-45º, 0º, 45º and A5 in the range of 0º - 90º. Franz et al., 2023.

3.2. Beam stabilization system on the USPLR system

The beam deviation reduces the processing accuracy of the system. A beam stabilization system is therefore developed to correct the beam position misalignment during the processing. The linear drift is corrected by the first mirror and first camera, followed by the correction of the angular drift (Further details are discussed in our previous research (Yang et al., 2023, 2025)).

In addition, a prolonged correction time was observed in instances of significant position deviation. The enhancement of the correction efficiency could be realized by refining the camera settings such as, e.g., exposure time and applying cameras with high framerate. As an evaluation, a three-layer neural network is applied to optimize the beam position stabilization

process, with which the correction time for the large beam misalignment is reduced to the half of the algorithm without neural network (Yang et al., 2025). The beam position deviation before and after beam stabilization is shown in Table 1. Please note that the beam deviation is represented in x and y direction and the defined calculation tolerance is 20 pixel for each direction.

Table 1. Beam position deviation before and after beam stabilization.

Position	Before / µm		After / µm		Correction rate / %
	Avg.	Std.	Avg	Std	
CAM3x	133.05	92.89	13.07	8.58	90.18
CAM3y	78.31	49.16	17.60	7.61	77.53
CAM4x	225.79	219.75	12.80	7.97	94.33
CMA4y	310.43	198.24	13.51	6.49	95.65

This system was applied additionally for the determination of the optimal beam alignment, with which a minimum beam position misalignment is induced during the system movement. Laser beam center is aligned to the set position at robot position A5 = 90º. Both cameras capture beam center position at three robot positions A5 = 0º, 45º and 90º. The center of mass for the three chosen robot positions are defined as the neu set position and laser beam is re-aligned to this position at robot position A5 = 90º. This process is repeated until the beam position deviation remains constant. As shown in Fig. 3(a), the center of mass moves inwards in a spiral trajectory and keeps turning around a circle with developing of the iterations. The position deviation in all directions reduced at the iteration from 1 to 8, and ultimately stabilized at a constant value from

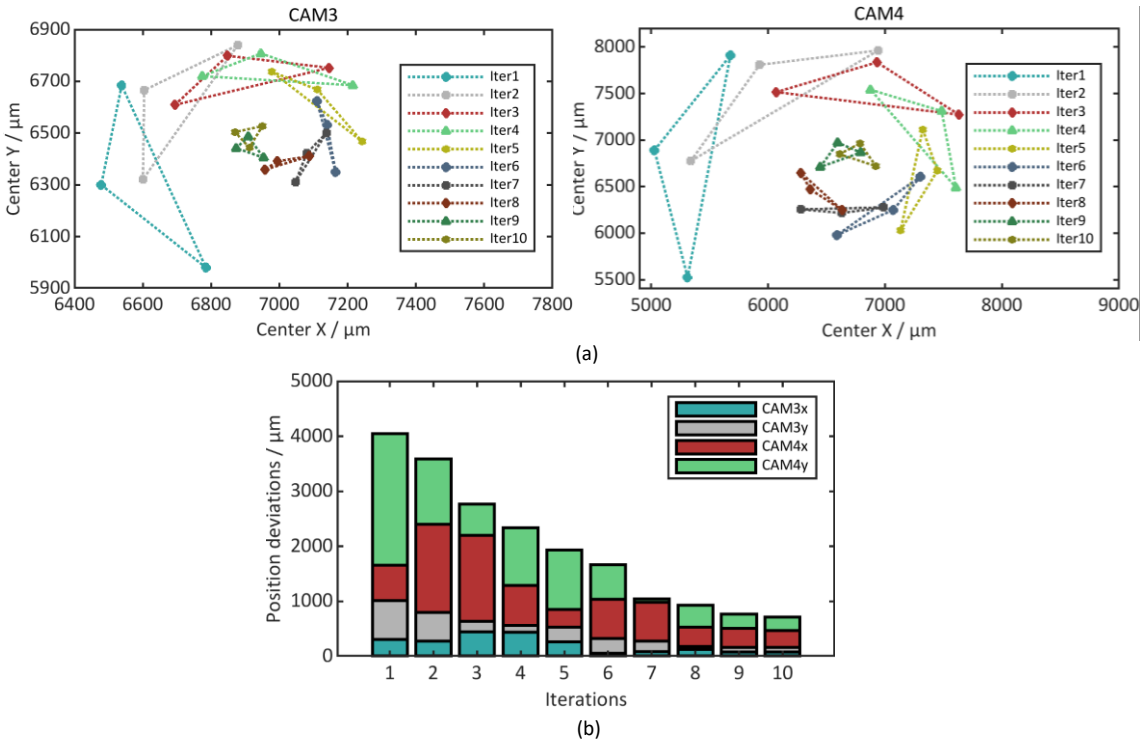

Fig. 3 Determination of optimal beam center position on CAM3 and CAM4 with designed system. (a) The position distribution of 10 iterations of the determination process; (b) Beam position deviation after each iteration.

iteration 9 onward (Fig. 3(b)). The determination process was paused after 10 iterations and the residual total position deviation was 719 µm, representing an 82.22% reduction of the initial total position deviation. Notably, the reduction of position deviation was 50 µm after 10 iterations, whereas it was 459 µm after only 2 iterations. A further reduction can be achieved by decreasing the defined tolerances and increasing the number of iterations.

Comparing the manual method introduced in our previous research (Franz et al., 2023), the present method utilizes motorized mirrors to re-align the beam and employs cameras to track the beam center position. This approach reduces the complexity of the beam adjustment process and enhances the process efficiency. This method demonstrates simplifying the operational procedure and the feasibility of in-situ quick beam re-alignment in the industrial production.

3.3. System performance

Overall, the robot enhances the system flexibility for micromachining using USP laser. The technical specifications of the robot are listed in Table 2. Defining the laser beam focus position as the TCP (Tool Center Point) (as shown in Fig. 4), a large 3D processing area is realized. The system rotation is based on the defined TCP in x, y, z direction. Consider the structure of A4 and A5, the processing area from the initial system position is defined in Table 3. Please note that, for remaining the constant position between the robot and scanner coordinate system, the extra rotation along z direction is not allowed.

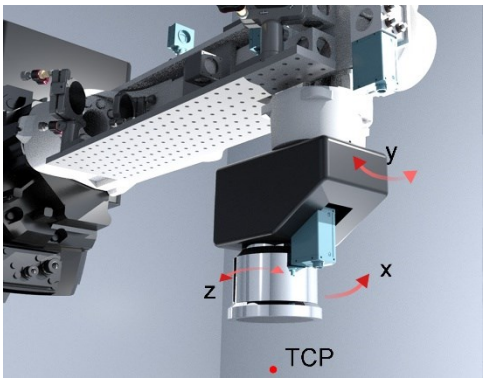

Fig. 4 TCP of the USPLR System. The rotation direction is based on the TCP. (Yang et al. 2025)

Table 2. System specifications of IRB 2600ID-8/2.00.

	Value	Unit
Handling capability	8	kg
Position repeatability	0.023	mm
Position accuracy	0.033	mm
Linear path repeatability	0.27	mm
Linear path accuracy	0.70	mm
Maximum axis speed A1-A3	175	º/s
Maximum axis speed A4-A5	360	º/s

Table 3. System processing area.

Directions	x*	y*	z*
Translocation / mm	[− 330,380]	[− 480,480]	[− 480,80]
Rotation / º	[0,20]	[− 15,15]	[0,0]

* The distance shown in the Table is based on the defined system initial position.

3.4. Micromachining with the USPLR system

The first realization of 2D and 3D micromachining using USPLR system is shown in Fig. 5. Multiple materials have been successfully processed by the USPLR system. A cut edge with a negligible heat affected zone is shown in the PET film cutting with a height difference of 35 mm (Fig. 5(a)). In addition, the USPLR system demonstrates a notable capability in glass processing. Fig. 5(c) involves a structuring process on the pyramid surface. The substrate was put on a table normally and robot rotated the axes until the laser beam propagating axis behind F-Theta lens was parallel to the normal of the processing surface.

The system due to high flexibility shows advantages on ultra-thin glass (UTG) cutting. Fig. 6 shows processing of 100 µm thickness AF eco 32 UTG. A large glass sample with a thickness of 100 µm and a width of 300 mm was cut out from a 300 mm×300 mm×100 µm UTG by the USPLR system, where the cut edge is free of cracks. A cutting and structuring combined process is illustrated in Fig. 6(b). A cloud-like complex structure with a length of 180 mm was cut out from the UTG glass sample following a structuring process in the middle.

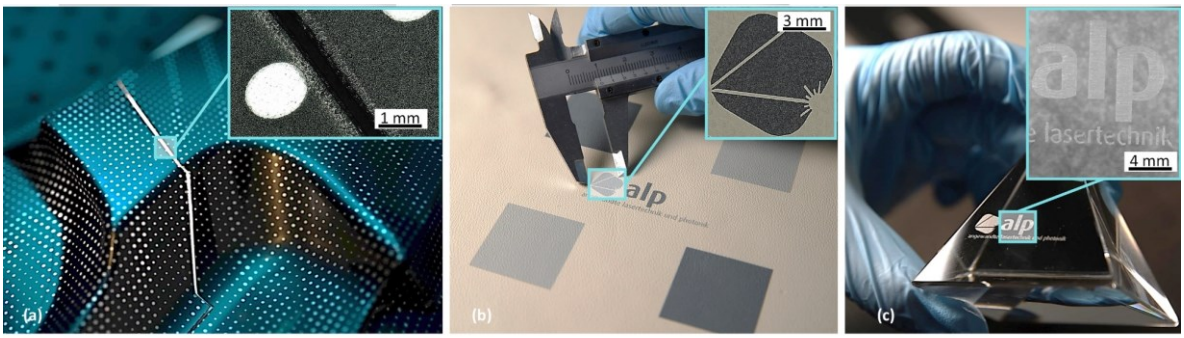

Fig. 5 Cutting, marking and structuring performed with the USPLR system for automotive dashboard applications and glass substrate. (a)PET film, (b) Leather, (c) Pyramid made of glass material. (Franz et al., 2023)

Furthermore, a real-3D cutting process of UTG is illustrated in Fig. 7. A 100 µm glass sample was bent and clamped between two holders. The beam focus was defined at the sample surface and monitored using a confocal sensor. During the process, the robot moved along the surface with remaining beam propagating axis behind F-Theta lens parallel to the surface normal of the bent glass sample. An offset between laser activation and the beginning of the robot movement as well as an offset between laser deactivation and the stop of robot movement avoids the influence of the robot acceleration and deceleration on the cutting quality.

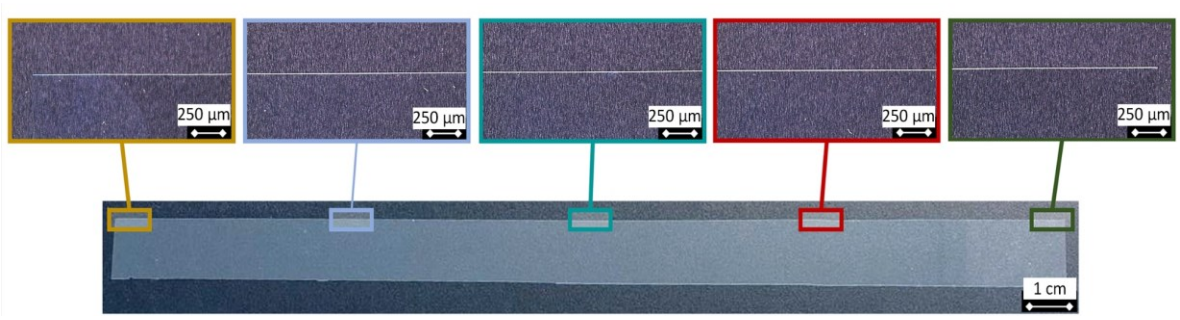

(a)

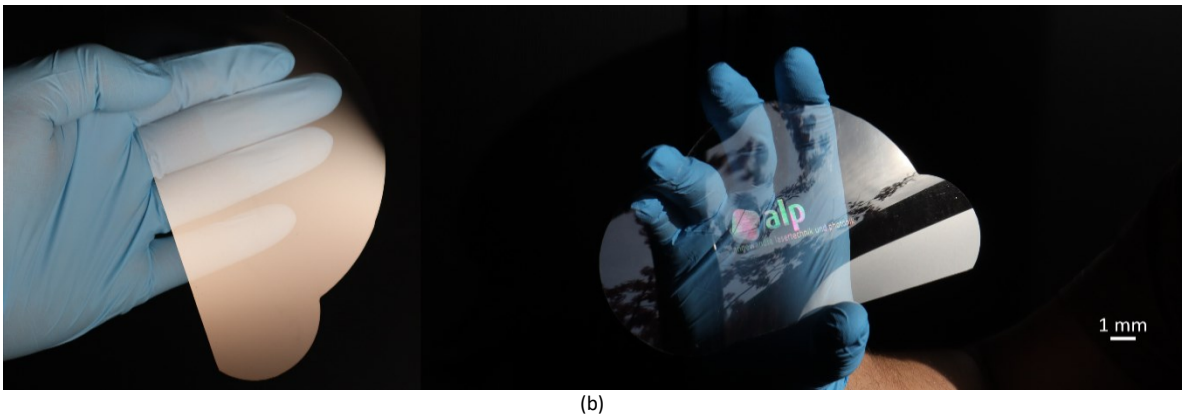

(b)

Fig. 6 Ultra-thin glass thru cutting. (a) Large area cutting. (b) Cutting with complex structure.

4. Conclusion

An ultrashort pulsed laser integrated on an articulated six axis robot named ultrashort pulsed laser robot system has been discussed in this contribution. The beam position deviation caused by the robot movement is suppressed by a beam stabilization system, which successfully corrected over 95% of the beam position misalignment after the robot movement. Furthermore, an automated optimal beam alignment determination method was introduced in this contribution, reducing

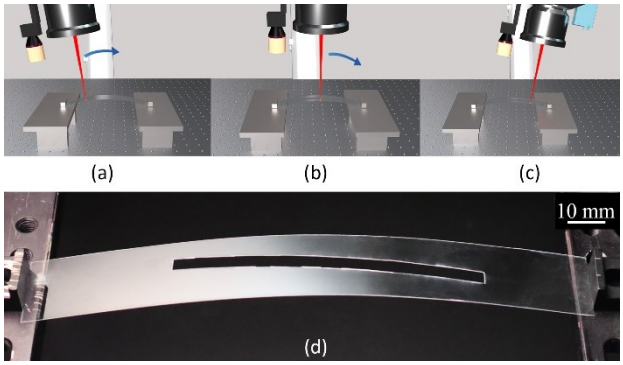

Fig. 7 Real-3D processing of UTG D263. The glass sample is bent and clamped between two holders. Robot moves along the curved surface with remaining the beam propagation axis behind F-Theta lens parallel to the normal of the processing surface.

over 82% of the initial beam position deviation after 10 iterations. This significantly simplifies the beam adjustment process for the system. The demonstrated 2D and 3D applications validate the system flexibility and highlight its potential for industrial-scale ultrashort pulsed laser processing.

Acknowledgements

This research was funded by the Bavarian Ministry of State for Economy, Land Development and Energy (project RoboSens, grant number DIK0375/01) and by the Bavarian Ministry of Science and Arts (project LEZ, grant number H.2-F1116.AS/34/2).

Publication bibliography

Batal, A., Michalek, A., Penchev, P., Kupisiewicz, A., Dimov, S., 2020. Laser processing of freeform surfaces: A new approach based on an efficient workpiece partitioning strategy. International Journal of Machine Tools and Manufacture 156, p. 103593.

Belle, S., Helfert, S. F., Kefer, S., Hellmann, R., Jahns, J., 2022. Space-variant polarization conversion with artificial birefringent metallic elements. Optics letters 47, pp. 2024–2027.

Bischoff, K., Kefer, S., Wienke, A., Overmeyer, L., Kaierle, S., Esen, C., Hellmann, R., 2023. Integration of Bragg gratings in aerosol-jetted polymer optical waveguides for strain monitoring capabilities. Optics letters 48, pp. 1778–1781.

Brodsky, A., Kaplan, N., 2022. 3D beam shaping methods for ultrashort ‐ pulsed laser material processing. PhotonicsViews 19, pp. 56 ‐ 59.

Franz, D., Häfner, T., Kunz, T., Roth, G.-L., Rung, S., Esen, C., Hellmann, R., 2022. Ultrashort Pulsed Laser Drilling of Printed Circuit Board Materials. Materials 15.

Franz, D., Yang, Y., Michel, L., Esen, C., Hellmann, R., 2023. Evaluation of an ultrashort pulsed laser robot system for flexible and large-area micromachining. Journal of Laser Applications 35, 042057.

Karkantonis, T., Penchev, P., Nasrollahi, V., Le, H., See, T. Long, Bruneel, D. et al., 2022. Laser micro-machining of freeform surfaces: Accuracy, repeatability and reproducibility achievable with multi-axis processing strategies. Precision Engineering 78, pp. 233–247.

Mishchik, K., 2016. Ultrashort Pulse Laser Cutting of Glass by Controlled Fracture Propagation. JLMN 11, pp. 66–70.

Raciukaitis, G., 2021. Ultra-Short Pulse Lasers for Microfabrication: A Review. IEEE J. Select. Topics Quantum Electron. 27, pp. 1–12.

Yang, Y., Franz, D., Esen, C., Hellmann, R., 2023. Development and comparison of algorithms for beam stabilization in ultrashort pulsed laser equipped on a six-axis robot. Journal of Laser Applications 35, 042039.

Yang, Y., Franz, D., Esen, C., Hellmann, R., 2025. Development of a dynamic beam stabilization system for a six-axis ultrashort pulsed laser robot. J Intell Manuf.

Zettl, J., Klar, M., Rung, S., Esen, C., Hellmann, R., 2021. Laser turning with ultrashort laser pulses. Journal of Manufacturing Processes 68, pp. 1562–1568.